JOURNAL OF THERMOPHYSICS AND HEAT TRANSFER
Vol. 15, No. 3, July–September 2001

Gas–Surface Interaction Model Influence on Predicted Performance of Microelectromechanical System Resistojet

Andrew D. Ketsdever*
U.S. Air Force Research Laboratory, Edwards Air Force Base, California 93524
Dean C. Wadsworth†
ERC, Inc., Edwards Air Force Base, California 93524
and
E. P. Muntz‡
University of Southern California, Los Angeles, California 90089

The free molecule micro-resistojet was designed as a micropropulsion system capable of performing attitude control and primary maneuvers for nanospacecraft with mass less than 10 kg. The details of gas–surface interactions between propellant molecules and surfaces held at elevated temperature are critical in predicting the propulsion system's performance and efficiency. The aim is to assess parametrically the performance of a typical thruster geometry using a general Maxwell scattering model and two versions of the Cercignani–Lampis–Lord model (Lord, R. G., "Some Extensions of the Cercignani–Lampis Gas–Surface Scattering Kernal," *Physics of Fluids, A*, Vol. 3, No. 4, 1991, pp. 706–710 and Lord, R. G., "Some Further Extensions of the Cercignani–Lampis Gas–Surface Interaction Model," *Physics of Fluids, A*, Vol. 7, No. 5, 1995, pp. 1159–1161). The models are incorporated into a direct simulation Monte Carlo numerical code and are used to bound the predicted performance characteristics of the thruster. The total specific impulse varies by approximately 20% over range of accommodation coefficients from specular to diffuse surface scattering. However, there was only a maximum difference of about 5% between the models for a given accommodation coefficient. Other more microscopic parameters, such as axial velocity distribution functions, appear to depend more on the scattering model assumed.

Nomenclature

A	=	area, m^2
a	=	accommodation coefficient
$\bar{c}'$	=	average thermal speed, m/s
g_0	=	gravitational constant, 9.80 m/s^2
I_{sp}	=	specific impulse, s
k	=	Boltzmann's constant, 1.38×10^{-23} J/K
m	=	mass, kg
$\dot{m}$	=	mass flow rate, kg/s
n	=	number density, m^{-3}
p	=	pressure, Pa
T	=	temperature, K
$\mathfrak{T}$	=	thrust, N
α	=	expansion slot angle
Δv	=	change in velocity, m/s
χ	=	probability that a molecule exits the expansion slot once it enters

Subscripts

i	=	propellant inlet
p	=	propellant
s	=	spacecraft
w	=	wall
0	=	stagnation region

Presented as Paper 2000-2430 at the AIAA 34th Thermophysics Conference, Denver, CO, 19–22 June 2000; received 28 July 2000; revision received 26 January 2001; accepted for publication 26 January 2001.

*Senior Research Engineer, Advanced Concepts Division, Propulsion Directorate, 10 E. Saturn Boulevard; andrew.ketsdever@edwards.af.mil. Senior Member AIAA.
†Research Scientist. Member AIAA.
‡A. B. Freeman Professor, Chair, Department of Aerospace and Mechanical Engineering. Fellow AIAA.

Introduction

THE free molecule micro-resistojet (FMMR) has been designed and developed as a primary and attitude control thruster for nanospacecraft (mass ≤ 10 kg) (Refs. 1 and 2). The FMMR is constructed using microelectromechanical systems (MEMS) fabrication techniques, which allows it to be machined on a micrometer scale and to be easily integrated with other MEMS components such as embedded control systems, valves, and pressure regulators. Although MEMS fabrication can be very beneficial to micropropulsion systems, a serious drawback of traditional MEMS micromachining is that only compatible materials can be used in the fabrication process, which can limit device performance. A schematic of the FMMR is given in Fig. 1.

The propellant gas enters into the FMMR stagnation region through a MEMS valve and filter assembly connected by the propellant inlets. The device operates at unusually low pressures (50–500 Pa), which gives the propellant gas molecules a mean free path on the order of the expansion slot width. With MEMS fabrication techniques, the slot size can be machined with a width as small as ~ 1 μm; however, the nominal FMMR geometry used in this study has a slot width $w = 100$ μm. Energy is imparted to the propellant gas through collisions with a thin-film heating element suspended above a silicon pedestal. The pedestals act to minimize direct line-of-sight propellant transport through an expansion slot after entering the stagnation region.

The design requirement is to arrange a surface held at an elevated temperature to be the last surface contacted by a propellant molecule before it exits the device through an expansion slot. This requirement suggests that the spacing between the thin-film heater and the expansion slot be on the order of the molecular mean free path in the device to reduce intermolecular collisions before expansion.

The FMMR relies on the transfer of energy into a propellant gas through molecular collisions with the heated surface. Because the thin-film heater is the only heated surface in the device, subsequent molecular collisions with relatively cold thruster surfaces are expected to be a major loss mechanism. For these reasons, the details of the gas–surface interaction are critical in predicting the propulsion

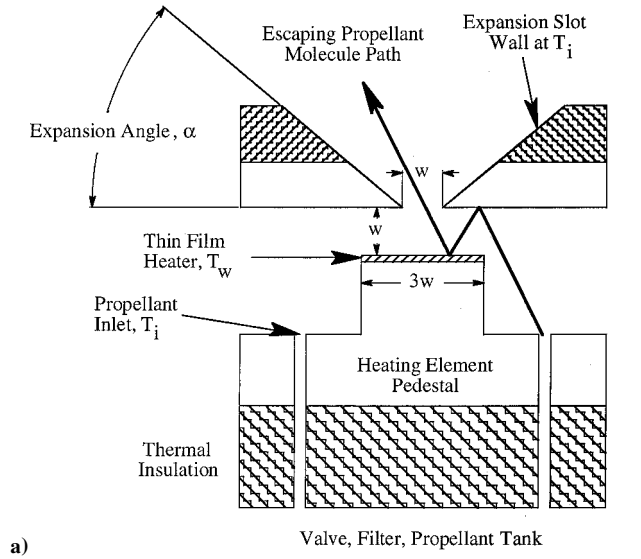

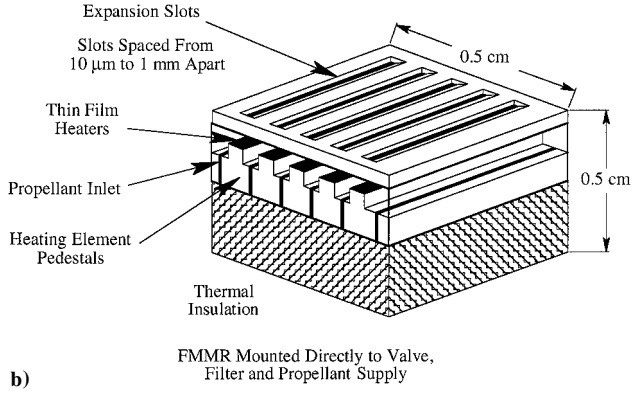

Fig. 1 FMMR conceptual design schematic: a) cross section of FMMR showing heating element arrangement with the expansion slot and b) multislot ($w = 100\ \mu$m) configuration with a 0.5 × 0.5 cm cross-sectional area.

system's performance and efficiency. The aim of this study is to assess parametrically the performance (thrust and specific impulse) of a typical FMMR geometry using several gas–surface interaction models. The models are incorporated into a direct simulation Monte Carlo (DSMC)[3] code to bound the predicted performance characteristics of the thruster.

Theory

In a uniform free molecule flow, the thrust $\mathfrak{J}$, or flux of normal momentum, produced by a gas at a stagnation pressure of p_0 through a thin orifice or slot of area A_0 is

$$\mathfrak{J} = \chi(p_0/2)A_0 = \chi(n_0 K T_0/2)A_0 \tag{1}$$

In the case of the FMMR, the stagnation temperature in the vicinity of the expansion slot is governed by the physics of the interaction between the propellant gas and the thin-film heated element. For the present study, the thin-film heated element is assumed to be an inert surface material defined by a wall temperature T_w and a single energy accommodation coefficient a. Therefore,

$$T_0 = aT_w + (1 - a)T_i \tag{2}$$

where the stagnation temperature is in the vicinity near the expansion slot. The free molecule mass flow through an infinitely thin orifice or slot is

$$\dot{m} = \chi m(n_0\bar{c}'/4)A_0 = \chi(mn_0/4)\sqrt{8kT_0/\pi m}\,A_0 \tag{3}$$

A propulsion system's efficiency is generally evaluated based on the thruster's intrinsic specific impulse or I_{sp}. The I_{sp} of a propulsion system is the ratio of the thrust generated to the propellant mass flow required to produce the thrust. For a free molecule flow through a thin orifice or slot the specific impulse is given by

$$I_{sp} = \frac{\sqrt{\pi kT_0/2m}}{g_0} \tag{4}$$

As evident in the preceding formulation, the details of the energy exchange between the thin-film heaters and propellant molecules drive the performance of the FMMR.

Calculations

The analytical, free molecule results from the preceding section are expected to be useful in the basic design of the FMMR; however, DSMC[3] calculations are required to predict flowfield properties of the actual FMMR under transitional rarefied flow conditions. Many of the input models required, such as gas–surface interaction, are topics of current research; however, parametric variation of the model features can be used to assess performance sensitivity to these uncertainties independently.

The two-dimensional computational domain for the nominal FMMR geometry is shown in Fig. 2. The geometry is symmetrical about the slot centerline IJ. Boundary AB is an open inlet; molecules entering are selected from a drifting equilibrium distribution at T_i, with the drift velocity iteratively updated to match the input plenum pressure at the boundary. Boundary CD is a plane of symmetry (assuming a multislot configuration). The far-field vacuum boundary DJ is placed approximately 10 slot widths downstream of the slot exit. Each wall surface is a reflector defined by an accommodation coefficient a and an input temperature, either T_i or T_w (surface FI only).

The key feature that enhances bulk flow in the propellant gas is the differential heating of the thin-film heater FI (at T_w) relative to that of the nominal plenum inlet and surface temperature (at T_i). In this study, all surfaces except the thin-film heater are assumed to be at the gas inlet temperature T_i. More accurate simulations would require iterative coupling of the gas and structural heat transfer properties.

The code is instrumented to sample directly and spatially resolve the flux of molecular mass, momentum, and energy through an arbitrary flowfield plane, here typically chosen to be the slot throat (GG′) or the slot exit (HH′). The code also samples the axial and transverse velocity distribution function at arbitrary locations, including surface boundaries, to allow more detailed comparison with the simple free molecule theory. In this manner, performance losses can be attributed to various components of the geometry such as the slot walls denoted by the line segment GH.

For the present highly rarefied operating conditions, the DSMC requirement that the nominal cell size be on the order of the local molecular mean free path and that the simulation time step be small relative to the mean collision time are easily met. The nominal simulation grid contained 2000 cells, with cell size typically much less than 25% of the local mean free path. The nominal time step was approximately 50% of the mean collision time.

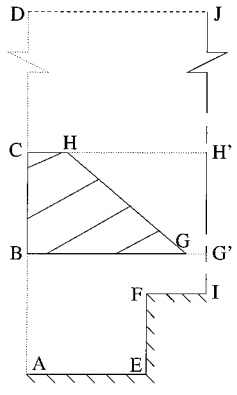

Fig. 2 FMMR computational geometry for DSMC calculations.

The simulations were run for 2000 unsteady and 10^4 additional steady-state time steps during which sampling of the flowfield occurred. The nominal simulation contained 2×10^5 particles at steady state, and flux plane sample sizes were 10^6. Statistical scatter in the predicted specific impulse, for example, is estimated to be much less than 1% due to the large sample sizes obtained.

Because experimental performance measurements of this device are unavailable, a large variety of sensitivity studies have been carried out to estimate simulation accuracy. The largest potential source of error in the present simulations is expected to be in the modeling of the gas–surface interaction process. For nonideal surfaces, parametric studies using the phenomenological models show variations in predicted specific impulse on the order of 5%.

For simplicity in these initial design studies, calculations have been made assuming an argon propellant, although it is far from an optimum choice for an electrothermal thruster. For more accurate performance predictions with realistic propellant molecules, the influence of internal modes must be addressed. The typical propellant inlet temperature and pressure are 300 K and 50 Pa, respectively. The nominal FMMR geometry has a slot width of $w = 100\ \mu$m, an expansion angle $\alpha = 40$ deg, and an expansion slot thickness of 250 μm. The inlet conditions and slot width yield a Knudsen number of unity.

Gas–Surface Interaction Models

Despite advances in micromachining technology, silicon and silicon-based materials are still the most common material used in MEMS fabrication. Exposure of pure silicon to potential propellant gases such as ammonia (NH_3) or water (H_2O) may lead to dissociative adsorption and subsequent nitridation or oxidation of the silicon surface even under benign conditions, for example, room temperature.[4] Very little information is available regarding their influence on macroscopic processes such as gas transport.[5] Molecular-level data indicate desorption is, in general, a highly nonequilibrium process,[6] further complicating model development.

As such for the present performance studies, an inert surface material defined by a wall temperature T_w or T_i and a single accommodation coefficient a are assumed. An estimate of the influence of the reflection (or desorption) process on overall performance is then made by comparative calculations for three models: the Maxwell model[3] and two forms of the Cercignani–Lampis–Lord (CLL) model.[7,8]

In the Maxwell model, a fraction a of incident particles fully accommodate to the wall temperature and are diffusely reflected with the remainder being specularly reflected. Molecular beam studies have shown that this model is not realistic, and that, in general, reflected molecules at a surface exhibit a lobular distribution in direction and a continuous spread in energy.

In the original form of the CLL model, reflection varies from specular ($a = 0$) to fully accommodating ($a = 1$) as with the Maxwell model.[7] However, the CLL original model allows for separate normal and tangential energy accommodation coefficients (which for simplicity are equivalent in this study). This form of the CLL model produces physically reasonable distributions of direction and energy for reflected molecules although it can not be used to describe discrete internal energy states of the molecule.

A generalized form of the CLL model provides for diffuse molecular reflection at a surface with incomplete energy accommodation.[8] The CLL diffuse model retains the energy distribution obtained from the original CLL model but removes the angular dependence for surface reflection (corresponding to diffuse reflection). Both the CLL original and CLL diffuse models are compared to the simple Maxwell model to assess the predicted FMMR performance.

In principle, the details of the energy deposition and desorption process can be directly incorporated into the DSMC gas–surface interaction procedure as they become available. For the present range of FMMR conditions, gas-phase processes such as recombination are negligible due to the low operating pressures. Therefore, the key parameters required for more detailed studies are the net velocities or translational energy components of the (potentially dissociated) products of the desorbing propellant molecule, rather than the specifics of the pathways by which the adsorption and decomposition occur.

Thermal Accommodation of Gases on Surfaces

An extensive literature exists detailing the measurements of the thermal accommodation coefficient for various gas–surface systems.[9–12] Although there have been a number of notable measurements made for monatomic or simple diatomic gases interacting with pristine metal surfaces, obtaining measurements and developing numerical models for complex flows on engineering surfaces is an area of active research.[13–16] With current MEMS fabrication practices, the thin-film heating element can either be made from a polysilicon material or sputter deposited metals such as platinum or gold. It is assumed for the purposes of this research that the heating element is a deposited platinum surface with a thickness of approximately 2000 Å.

The temperature-dependent accommodation coefficient depends on several factors including the physical characteristics of the gas, the solid surface, the surface temperature, and the gas temperature. From previous research, the accommodation coefficient for argon impacting a platinum surface at thermal energies ranges from 0.71 (Ref. 9) to 0.9 (Ref. 11) at $T_w = 300$ K. At the FMMR operating temperature of $T_w = 600$ K, the accommodation coefficient ranges from 0.5 (Ref. 10) to 0.63 (Ref. 11). Accommodation coefficient data for argon colliding with a silicon surface, which are needed to estimate the energy losses on the expansion walls, are not available.

Because of uncertainties in the experimental measurements and in some cases a complete lack of data, the calculations presented in the following section include full parametric analysis with the accommodation coefficient. For simplicity, the accommodation coefficients of a given case are assumed to be equivalent for both the thin-film heater and the expansion walls. Despite these difficulties, the experimentally derived accommodation coefficients can be used as a general guideline in assessing predicted FMMR performance.

Results

Baseline estimates of the FMMR performance, that is, thrust and specific impulse, and flowfield behavior were obtained assuming a Maxwell surface model with complete accommodation ($a = 1$) using an argon propellant. At full accommodation, the Maxwell and both versions of the CLL model are equivalent. Figure 3 shows the FMMR flowfield contours for complete surface accommodation with $T_w = 600$ K. The contours show the gas translational temperature on the left side and axial velocity on the right side. In the slip layer (of characteristic dimension one mean free path) above the heated surface, the local gas state will comprise two basic classes of molecules, those directed away from the wall (and whose last collision event was with the wall) and those directed toward the wall. In the three-dimensional free molecule case, this latter class will contain molecules whose last collision was with another, cooler surface. For the present, finite Knudsen number conditions ($Kn \sim 1$), this class will also include molecules that have undergone intermolecular collisions with the cooler ambient gas. Macroscopically,

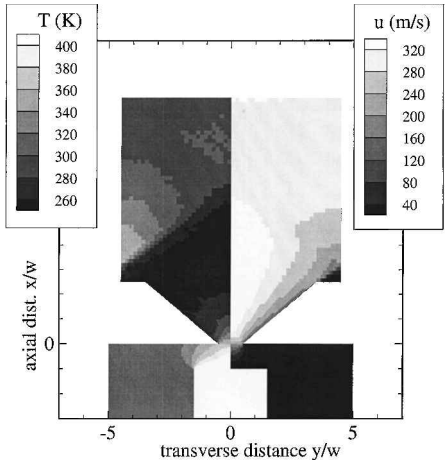

Fig. 3 Flowfield contours for nominal operating conditions: translational temperature (left) and axial velocity (right).

this complex nonequilibrium phenomenon is described as temperature slip and is clearly observed in the temperature contours, where the peak temperature in the gas near the heated surface remains much lower than T_w. Figure 4 compares the calculated specific impulse with the theoretical value [Eq. (4)] as a function of the heated wall temperature. For the nominal case, the corresponding thrust per unit expansion slot length is nearly 2.5 mN/m.

The molecular velocity distribution function available directly from the DSMC calculations provides a means to quantify the local degree of translational nonequilibrium in the gas. Figure 5 shows the centerline axial velocity distribution function at the expansion slot exit (H′ in Fig. 2) and throat (G′ in Fig. 2) for the nominal case using the Maxwell model with $a = 1$. The theoretical one-dimensional free molecule axial velocity distribution function at the expansion slot exit would consist of a half-Maxwellian evaluated at T_w. Obviously, the flowfield at the exit differs from the simple free molecule analysis; however, the comparisons in Fig. 4 suggest that the simple model can serve well for initial performance studies.

Figure 6 shows the net axial force along the expansion slot walls for various expansion angles α. For these results, the heated wall temperature is $T_w = 600$ K and the expansion slot wall temperature is $T_i = 300$ K with full surface accommodation. The net increase or decrease in thrust contributed by the expansion walls is given by the integrals under the curve in Fig. 6. For the convention used in Fig. 6, a positive integral implies thrust enhancement whereas a negative integral implies thrust degradation. For $\alpha = 40$ and 54.74 deg, the expansion walls contribute a net positive increment to performance by limiting divergence losses. Note that for $\alpha = 40$ and 54.74 deg the enhancement is maximized near the throat indicating that thin expansion slots are preferred. As the expansion angle increases for a fixed slot thickness, the shear forces begin to dominate and can significantly degrade the thruster's performance as seen for $\alpha = 90$ deg. From this analysis, relatively thin expansion walls with expansion angles $\alpha \leq 60$ deg are desirable. The expansion angle of 54.74 deg corresponds to that which can be etched by an isotropic wet chemical etchant along the ⟨100⟩ plane of crystalline silicon.

As mentioned earlier, the characteristics of the FMMR flowfield and performance are expected to depend on the details of the gas–surface interaction process. Figure 7 shows the specific impulse of the FMMR as a function of the surface accommodation coefficient for the Maxwell and the two versions of the CLL model. As Fig. 7 indicates, the models differ by only a few percent at a given accommodation. The accommodation coefficient in this case is assumed to be independent of the heated surface temperature; with this assumption, the peak specific impulse occurs for $a = 1$. The difference between the DSMC predictions and the free molecule theory lies in the effects of the expansion slot walls on the FMMR performance. As indicated in Fig. 6, the expansion slot walls act to improve the performance for small expansion angles. Because the free molecule theory is only truly valid for an infinitely thin orifice expansion, the effect of the slot walls is not accounted for in the theoretical results shown in Fig. 7.

Normalized specific impulse profiles across the slot expansion exit plane (HH′ in Fig. 2) for various conditions are shown in Fig. 8. As expected, the maximum specific impulse contribution is on the

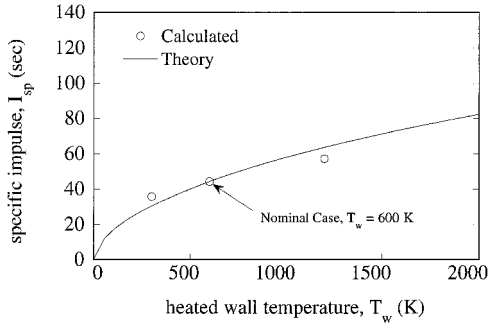

Fig. 4 FMMR performance as a function of operating temperature; theoretical line from Eq. (4).

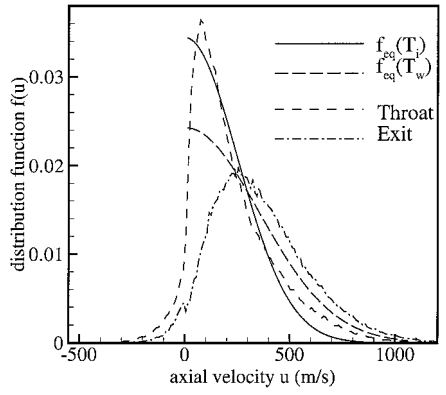

Fig. 5 Centerline axial velocity distribution function at the expansion slot throat and exit.

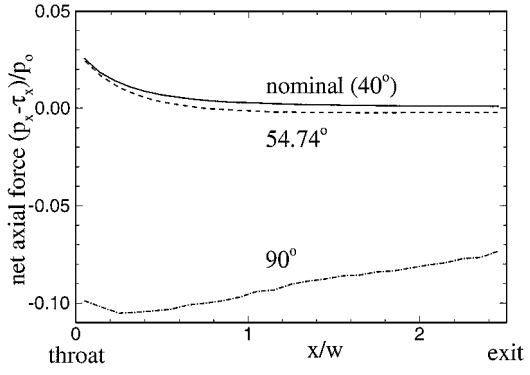

Fig. 6 Axial force contribution along the slot for various expansion angles.

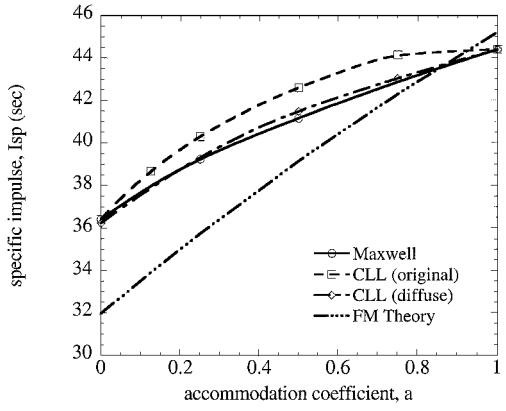

Fig. 7 Surface model effect on the predicted FMMR performance.

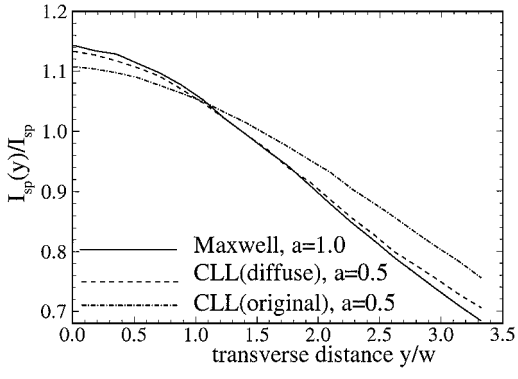

Fig. 8 Effect of the surface model on normalized specific impulse profile across expansion slot exit.

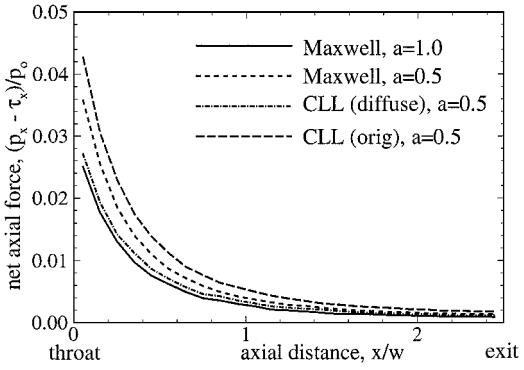

Fig. 9 Axial force contribution along the slot for various gas–surface interaction models.

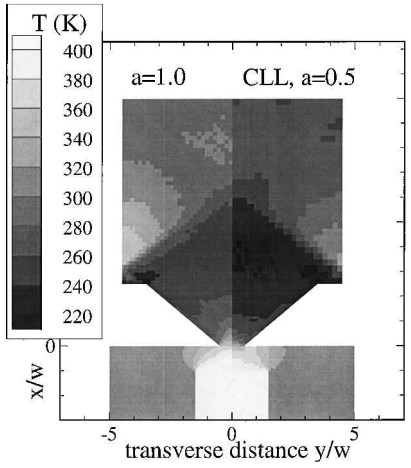

Fig. 10 Effect of the surface model on flowfield temperatures.

FMMR centerline, where losses due to the transverse velocity and collisions with the expansion walls are minimized. The specific impulse drops approximately 30% from the centerline value as the expansion walls are approached. Interestingly, it appears that the nature of the scattering process has a larger effect on the profile shape than does the magnitude of the accommodation.

Figure 9 shows the influence of the surface models on the net axial force along the expansion slot wall for $\alpha = 40$ deg. This effect is larger than that due to modest variations in the expansion slot angle about the nominal value shown in Fig. 6. Figure 9 also indicates that the scattering process contributes significantly to the determination of the optimal slot expansion length. To minimize shear and heat transfer to the expansion slot, thin expansion slots are desired. However, the benefit of redirecting errant molecules in the useful thrust direction is improved for thicker slots.

The FMMR flowfield temperature contours for full accommodation and for the CLL diffuse model with $a = 0.5$ are shown in Fig. 10. As expected, the temperature profile near the heated wall surface shows less energy is transferred into the propellant gas under incomplete accommodation conditions.

The major performance loss mechanism is expected to be caused by heated propellant molecules colliding with relatively cold thruster walls, particularly in the expansion region. Figure 11 shows the propellant heat flux as a function of axial distance x along the FMMR expansion slot. The upstream entrance to the slot (analogous to a nozzle throat) is $x/w = 0$. The integrals under the curves in Fig. 11 vary from 8.06×10^{-6} (Maxwell) to 9.38×10^{-6} kW/m (CLL diffuse) indicating that there is only about a 20% deviation between the gas–surface interaction models for a given accommodation. Therefore, the heat flux to the expansion wall appears to be relatively insensitive to the scattering model assumption.

As expected, the heat flux to the expansion walls increases with the accommodation coefficient as shown in Fig. 12. This influence

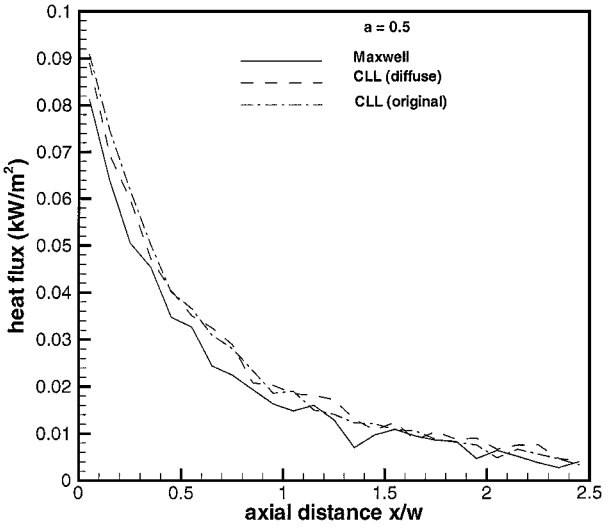

Fig. 11 Expansion wall heat flux for various gas–surface interaction models.

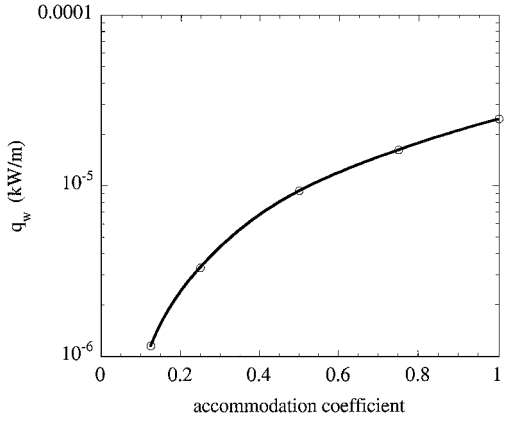

Fig. 12 Integrated heat flux per unit slot length to the expansion walls as a function of the accommodation coefficient for the CLL original model.

is larger in magnitude than that caused by varying the interaction model for a given accommodation coefficient (Fig. 11). Again, it is assumed that the accommodation coefficient is the same for all gas–surface collisions, that is, independent of gas and surface temperature, throughout a given simulation. Although these results are for the CLL original model, similar trends are seen with the other surface interaction models used in this study.

Discussion

As shown in Fig. 7, the details of the gas–surface interaction are important in effectively determining the predicted performance of the FMMR. As more appropriate propellants are investigated such as water vapor,[1] the physics of surface interactions will become increasingly complicated by adsorption, dissociation, and internal energy state excitation. Currently, adequate models are not available to address these interactions.

The mass of propellant required to perform a series of spacecraft orbital maneuvers is given by

$$m_p = m_s[\exp(\Delta v / I_{sp} g_0) - 1] \tag{5}$$

where m_s is the dry spacecraft mass, that is, without propellant, and Δv is the change in velocity that the propulsive maneuvers afford. A Δv of approximately 100 m/s is typical for a nanospacecraft mission ($m_i = 10$ kg), where the micropropulsion system is used for attitude control over the mission lifetime. Figure 13 shows the propellant mass required for the assumption above over the range of FMMR predicted I_{sp} shown in Fig. 7.

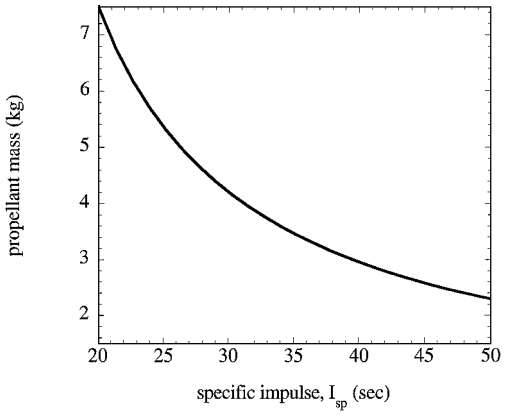

Fig. 13 Mission-required propellant mass as a function of FMMR performance.

As Eq. (5) indicates, an error in estimating the specific impulse can lead to larger errors in predicting the required propellant mass for a spacecraft mission due to the exponential term. For this reason, improved gas–surface interaction models and validating data are required to accurately estimate mission parameters.

Conclusions

It has been shown that the predicted performance of the FMMR depends on the details of the gas–surface interaction process used in the DSMC predictions. In general, the macroscopic properties of the FMMR (specific impulse, expansion slot axial force, and heat flux) appear to be more sensitive to the assumed magnitude of the accommodation coefficient than to the details of the surface scattering. The total specific impulse varies by approximately 20% over the maximum theoretical range of accommodation coefficients (zero to complete accommodation). However, there was only a maximum difference of about 5% between the models for a given accommodation coefficient. Other more microscopic parameters, such as the molecular velocity distribution function of the gas near the surface, appear to depend more on the scattering model assumption. These variations will be important in assessing the contamination potential of the micropropulsion system on nanosatellite missions.

The predicted performance of the FMMR, assuming a uniform, constant level of accommodation throughout the device, is maximized for full thermal accommodation. Proper selection of the material used on each component may further increase the performance of the device. For example, the use of a thin-film heater material that provides full thermal accommodation while choosing a more specular surface for the expansion slots would be beneficial. The overall thruster efficiency would be enhanced by allowing maximum energy input into the gas and minimizing the losses on the expansion slot walls.

Additional data are needed for the accommodation coefficient of gases on MEMS engineering surfaces such as silicon (single and polycrystalline), silicon oxide, silicon nitride, silicon carbide, and certain polymers. The gas–surface interaction models used in this study are still phenomenological. More physical models are required for calculations that simulate realistic propellants (typically stored as liquid) interacting with surfaces at elevated temperature. Additionally, the details of molecular scattering, adsorption (physi- and chemi-), desorption, dissociation, and internal energy mode coupling must be addressed.

References

[1]Ketsdever, A. D., Wadsworth, D. C., Vargo, S. E., and Muntz, E. P., "The Free Molecule Micro-Resistojet: An Interesting Alternative to Nozzle Expansion," AIAA Paper 98-3918, July 1998.

[2]Ketsdever, A. D., Wadsworth, D. C., and Muntz, E. P., "Predicted Performance and Systems Analysis of the Free Molecule Micro-Resistojet," *Micropropulsion for Small Spacecraft*, edited by M. Micci and A. Ketsdever, Vol. 187, Progress in Astronautics and Aeronautics, AIAA, Reston, VA, 2000, pp. 167–183.

[3]Bird, G., *Molecular Gas Dynamics and the Direct Simulation of Gas Flows*, Clarendon, Oxford, England, U.K., 1994, pp. 208–215.

[4]Dillon, A. C., Gupta, P., Robinson, M. B., Bracker, A. S., and George, S. M., "FTIR Studies of Water and Ammonia Decomposition on Silicon Surfaces," *Journal of Electron Spectroscopy Related Phenomena*, Vol. 54–55, 1990, pp. 1085–1095.

[5]Lundstrom, L., Norberg, P., and Petersson, L.-G., "Wall-Induced Effects in Gas Transport Through Micromachined Channels in Silicon," *Journal of Applied Physics*, Vol. 76, No. 1, 1994, pp. 142–147.

[6]Comsa, G., "The Dynamical Parameters of Desorbing Molecules," *Dynamics of Gas–Surface Interaction*, edited by G. Benedek and U. Valbusa, Springer-Verlag, New York, 1982, pp. 117–127.

[7]Lord, R. G., "Some Extensions to the Cercignani–Lampis Gas–Surface Scattering Kernal," *Physics of Fluids, A*, Vol. 3, No. 4, 1991, pp. 706–710.

[8]Lord, R. G., "Some Further Extensions of the Cercignani–Lampis Gas-Surface Interaction Model," *Physics of Fluids, A*, Vol. 7, No. 5, 1995, pp. 1159–1161.

[9]Yasumoto, I., "Accommodation Coefficients of Helium, Neon, Argon, Hydrogen and Deuterium on Graphitized Carbon," *Journal of Physical Chemistry*, Vol. 91, No. 16, 1987, pp. 4298–4301.

[10]Mann, W. B., "The Exchange of Energy Between a Platinum Surface and Gas Molecules," *Proceedings of the Royal Society of London, Series A: Mathematical and Physical Sciences*, Vol. 146, Oct. 1934, pp. 776–791.

[11]Thomas, L. B., and Olmer, F. G., "The Accommodation Coefficients of He, Ne, A, H_2, D_2, O_2, CO_2, and Hg on Platinum as a Function of Temperature," *Journal of the American Chemical Society*, Vol. 65, June 1943, pp. 1036–1043.

[12]Roach, D. V., and Thomas, L. B., "Comparative Study of Accommodation Coefficients of Helium and Neon on Clean Tungsten Under Transition, Temperature Jump, and Free Molecule Conditions," *Journal of Chemical Physics*, Vol. 59, No. 6, 1973, pp. 3395–3402.

[13]Goodman, F. O., and Wachman, H. Y., "Formula for Thermal Accommodation Coefficients," *Journal of Chemical Physics*, Vol. 46, No. 6, 1967, pp. 2376–2386.

[14]Chapovsky, P. L., van Duijn, E. J., Nagels, B., Cornelisse, L. N., and Hermans, L. J. F., "New Approach to Study the Molecular Internal to Translational Energy Transfer in Surface Collisions," *Rarefied Gas Dyanamics, Proceedings of the 19th International Sysmposium*, edited by J. Harvey and G. Lord, Oxford Univ. Press, Oxford, England, U.K., 1995, pp. 960–966.

[15]Borisov, S. F., and Polyckarpov, P. J., "An Experimental Study of the Momentum Accommodation in a Gas–Solid Body Problem," *Rarefied Gas Dynamics, Proceedings of the 20th International Sysmposium*, edited by C. Shen, Peking Univ. Press, Beijing, 1997, pp. 387–391.

[16]Hurlbut, F. C., "Two Contrasting Modes for the Description of Wall–Gas Interactions," *Rarefied Gas Dynamics*, edited by B. Shizgal and D. Weaver, Vol. 158, Progress in Astronautics and Aeronautics, AIAA, Reston, VA, 1994, pp. 494–506.